SEMINAR 1

COHERENT BACKSCATTERING AND WEAK LOCALIZATION PHENOMENA IN OPTICS AND IN METALS: ANALOGIES AND DIFFERENCES

R. MAYNARD, E. AKKERMANS* and P.E. WOLF

CNRS-CRTBT, BP 166X, 38042 Grenoble Cedex, France

Contents

It has by now been established that the electronic transport coefficients, like the electronic diffusion constant or the electronic conductivity, in weakly disordered metals† depart from the classical Boltzmann-type

* Also at Institut Laue-Langevin, BP 156X, 38042 Grenoble Cedex, France.

† By weakly disordered we mean that the wavelength at the Fermi level, λ_F, is much shorter than the elastic mean free path l. It means that we can make a perturbation expansion based on spherical waves for the eigenmodes, which is a good approximation as long as the ratio λ_F/l is small.

J. Souletie, J. Vannimenus and R. Stora, eds
Les Houches, Session XLVI, 1986—Le hasard et la matière/Chance and matter

theory. The well-known quantum correction originates from an interference effect along each closed diffusion path, which arises at the lowest order in λ_F/l, where λ_F is the Fermi wavelength and l the elastic mean free path. This is the so-called "weak localization" regime described in Course 4 by Ramakrishnan. The same interference phenomenon with "classical" waves (e.g. light or possibly sound) is expected in disordered media [1]. Recent experiments [2] exhibit a sharp peak in the angular dependence of the reflection coefficient (albedo) of a semi-infinite medium consisting of a suspension of polystyrene beads. When the sample is frozen, the albedo is very noisy and reveals [3] the well-known (in optics) speckle pattern of intensity. The angular correlation of this pattern is given by the ratio λ/D, where D is the width of the incident beam. In this note we will present the main features of the albedo of disordered media and we will emphasize at each stage of the analysis the analogies and differences between electromagnetic waves and electrons.

1. Elastic single scattering

In metals, the impurities or defects can give rise to elastic scattering, i.e., only the wavevector and not the energy changes. At the scale of the Fermi wavelength, the scatterers are often assumed to be point scatterers, leading to an isotropic cross section.

Single scattering of light is controlled by the ratio of the wavelength λ to the characteristic size of the scatterers as well as by the dielectric contrast between the particle and the medium. If $\lambda \gg d$, the scattering is of the Rayleigh type [$l(\omega) \propto \omega^{-4}$ in three dimensions], while the opposite case of short wavelength, $\lambda \ll d$, gives very anisotropic scattering tending to forward scattering. An exact expression for the scattering cross section exists for particles of spherical shape and is called Mie scattering.

2. Multiple scattering and ensemble average in concentrated solutions of scatterers

The single scattering approximation developed above describes the scattering properties of disordered media as long as the elastic mean free path is larger than the dimensions of the scattering volume. If the concentration of scatterers increases, this approximation breaks down and one is dealing with a multiple scattering problem. This is the common situation for electrons in disordered metals and for propagation of waves in the atmosphere or aerosols, in which the waves experience many scattering events before emerging. The transport properties of such media are usually described by means of a transport equation analogous to the Boltzmann equation (see, e.g., ref. [4]). Solved in the diffusion approximation (random walk of the intensity in the medium), one recovers, for example, the reflection and transmission coefficients of a slab of width L:

$$R = 1 - l/L, \qquad T = l/L, \tag{1}$$

where l is the elastic or transport mean free path introduced above. These relations are of course valid in the multiple scattering approximation, i.e., when $L \gg l$. But it is important to realize that such an approach is only valid on average, i.e., when the mean value is taken over all realizations of the distributions of scatterers. Such an average procedure eliminates accidental interferences, which are at the origin of the speckle pattern. These fluctuations of the reflection coefficient have been observed recently in the multiple scattering situation [3] in a frozen substance like a "fluff" of SiO_2 beads in air or $BaSO_4$ microparticles. Experimentally, averaging out the speckle pattern can be performed in different ways, e.g. numerical sampling average, rotation of sample. In another case, the brownian motion of latex colloidal particles in water suspension produces an ensemble self-averaging procedure for the reflected intensity as long as the time of exposure is longer than the characteristic time of motion of a particle over a wavelength (typically 10^{-3} s). The fluctuations recently observed in electronic microcircuits (for a review, see ref. [5]) on frozen disorder by varying the Fermi level or the magnetic field seem to be very similar to the speckle pattern.

3. Coherent and incoherent multiple scattering: the factor 2

Up to now, the transport properties of disordered media have been described by means of a Boltzmann-type transport equation. This approach neglects any wave character of the problem, except the λ-dependence of the elastic mean free path. In an average medium, the intensity at a given point is the sum of the intensities associated with the different multiple scattering paths arriving at this point. The very rapid variation of the phase associated with each of these paths gives the classical approximation a strong basis (see, e.g., ref. [4]). But it is only recently, in the context of electronic disordered media, that an interference effect which survives at the macroscopic scale to the average over the disorder has been found [6].

Let us be more explicit and define by $A(\boldsymbol{r}_0, \boldsymbol{r}_1, \ldots, \boldsymbol{r}_N, \boldsymbol{r})$ the complex amplitude at $\boldsymbol{r}$ after a multiple scattering sequence $\boldsymbol{r}_0, \boldsymbol{r}_1, \boldsymbol{r}_2, \ldots, \boldsymbol{r}_N, \boldsymbol{r}$, starting at $\boldsymbol{r}_0$. To obtain the total complex amplitude to go from $\boldsymbol{r}_0$ to $\boldsymbol{r}$, we have to sum over all the multiple scattering paths $(\boldsymbol{r}_1, \boldsymbol{r}_2, \ldots, \boldsymbol{r}_N) = \mathscr{C}_N$ of any length N and for all the scatterers. This complex amplitude $\gamma(\boldsymbol{r}_0, \boldsymbol{r})$ is given by

$$\gamma(\boldsymbol{r}_0, \boldsymbol{r}) = \sum_{N=1}^{\infty} \int_V \prod_{i=1}^{N} \mathrm{d}^3 r_i \, A(\boldsymbol{r}_0, \boldsymbol{r}, \mathscr{C}_N). \tag{2}$$

It must be noted that no boundary effect has been introduced and the previous relation is valid for an infinite medium.

Suppose now that the incident wave vector at $\boldsymbol{r}_0$ is $\boldsymbol{k}_0 = (2\pi/\lambda)\hat{\boldsymbol{s}}_0$ and the emergent wave vector at $\boldsymbol{r}$ is $\boldsymbol{k} = (2\pi/\lambda)\hat{\boldsymbol{s}}$. Then in the quasi-classical limit we define the complex amplitude $A(\boldsymbol{r}_0, \hat{\boldsymbol{s}}_0; \boldsymbol{r}, \hat{\boldsymbol{s}})$ to go from $\boldsymbol{r}_0$ with $\hat{\boldsymbol{s}}$ to $\boldsymbol{r}$ with $\hat{\boldsymbol{s}}$ as

$$A(\boldsymbol{r}_0, \hat{\boldsymbol{s}}_0; \boldsymbol{r}, \hat{\boldsymbol{s}}) = \mathrm{e}^{\mathrm{i}k(\hat{\boldsymbol{s}}_0 \cdot \boldsymbol{r}_0 - \hat{\boldsymbol{s}} \cdot \boldsymbol{r})} \gamma(\boldsymbol{r}_0, \boldsymbol{r}). \tag{3}$$

In order to illustrate eq. (3), let us consider the double scattering situation pictured in fig. 1. The incident plane wave $\mathrm{e}^{\mathrm{i}\boldsymbol{r}_0 \cdot \boldsymbol{r}_0}$ on the first scattering center $\boldsymbol{r}_0$ is scattered in the momentum state $\boldsymbol{k}_1$ and the second scattering center $\boldsymbol{r}$ diffuses it into the emerging plane wave $\mathrm{e}^{\mathrm{i}\boldsymbol{k} \cdot \boldsymbol{r}}$. The phase of the wave field after this sequence is

$$\varphi = (\boldsymbol{k}_1 - \boldsymbol{k}_0) \cdot \boldsymbol{r}_0 + (\boldsymbol{k} - \boldsymbol{k}_1) \cdot \boldsymbol{r}. \tag{4}$$

In order to calculate the associated intensity, we have to study two different physical situations, usually represented by the so-called ladder and crossed diagrams (cf. Course 4 by Ramakrishnan). The expression of the intensity is obtained by taking the squared modulus of the amplitude associated with the scattering sequence, i.e., $I = AA^*$. Instead of

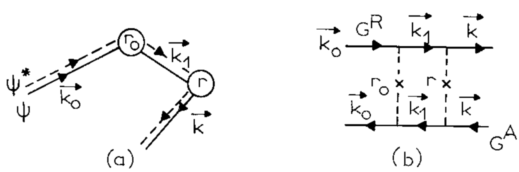

Fig. 1. (a) The double scattering sequence in real space. $\boldsymbol{r}_0$ and $\boldsymbol{r}$ denote the position of the scattering centers, while ψ and ψ^* represent the amplitude of the scalar wave field (e.g. electric field) and its conjugate, respectively. (b) The same scattering situation as described in (a), but in the Feynman diagram language using the propagators G^{R} associated with ψ and G^{A} associated with ψ^*.

representing this double scattering by the conventional diagrams in k-space involving advanced and retarded Green's functions, we prefer to draw the same sequence of scatterings in real space, where the Green's functions are represented by the field and conjugate field propagation (cf. figs. 1 and 2). The two different physical situations can then be described in the following way.

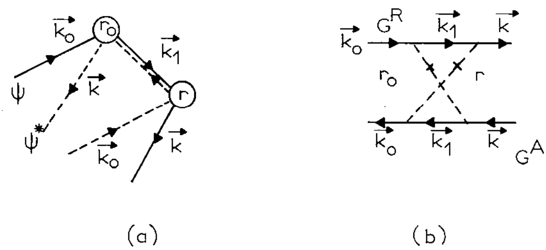

Fig. 2. (a) The coherent term is obtained when the two conjugate fields ψ and ψ^* are incident on different scattering centers. The phase difference is given by the scalar product of the transfer wave vector $(\boldsymbol{k}+\boldsymbol{k}_0)$ and $\boldsymbol{r}-\boldsymbol{r}_0$. (b) Crossed Feynman diagram which underlies the coherent effect.

3.1. Ladder diagrams

The two wave fields are propagating in the same direction. Therefore, they scatter on the two impurities in the same order. The phase of the conjugate wave field after the scattering sequence is

$$\varphi_L^* = -(\boldsymbol{k}_1 - \boldsymbol{k}_0) \cdot \boldsymbol{r}_0 - (\boldsymbol{k} - \boldsymbol{k}_1) \cdot \boldsymbol{r}. \tag{5}$$

In the expression of the intensity, these phases φ_L^* and φ cancel and we obtain the usual incoherent double scattering. This situation is depicted in fig. 1a in real space and in reciprocal space in fig. 1b as a ladder diagram.

3.2. Crossed diagrams

Suppose now that the conjugate wave field is incident on the second scattering center $\boldsymbol{r}$ so that it follows the same scattering sequence but in opposite order. The phase of the conjugate wave field after this reversed sequence is

$$\varphi_C^* = -(\boldsymbol{k}_1 + \boldsymbol{k}_0) \cdot \boldsymbol{r} + (\boldsymbol{k} + \boldsymbol{k}_1) \cdot \boldsymbol{r}_0. \tag{6}$$

In this case, in the expression of the intensity a phase factor remains, which is given from eqs. (4) and (6) by

$$\Delta\varphi = (\boldsymbol{k}+\boldsymbol{k}_0)\cdot(\boldsymbol{r}-\boldsymbol{r}_0). \tag{7}$$

This situation is depicted in fig. 2a in real space and its equivalent in reciprocal space is represented in fig. 2b as a crossed diagram.

A straightforward generalization of the double scattering situation is provided by eq. (3), where $\gamma(\boldsymbol{r}_0, \boldsymbol{r})$ represents the amplitude at point $\boldsymbol{r}$ for all the sequences starting at $\boldsymbol{r}_0$. The same analysis in terms of ladder and crossed diagrams remains and one obtains the conclusion: in the ladder configuration, the intensity is given by $\mathrm{Re}(AA_\mathrm{L}^*)$, where A is given by eq. (3) and

$$A_\mathrm{L}^*(\boldsymbol{r}_0, \hat{\boldsymbol{s}}_0; \boldsymbol{r}, \hat{\boldsymbol{s}}) = \mathrm{e}^{-\mathrm{i}k\hat{\boldsymbol{s}}_0\cdot\boldsymbol{r}_0}\gamma^*(\boldsymbol{r}_0, \boldsymbol{r})\,\mathrm{e}^{\mathrm{i}k\hat{\boldsymbol{s}}\cdot\boldsymbol{r}},$$

so that $I_\mathrm{inc} = |\gamma(\boldsymbol{r}_0, \boldsymbol{r})|^2$, i.e. the usual incoherent contribution.

In the crossed configuration, the intensity is given by $\mathrm{Re}(AA_\mathrm{C}^*)$, where now

$$A_\mathrm{C}^*(\boldsymbol{r}, \hat{\boldsymbol{s}}_0; \boldsymbol{r}_0, \hat{\boldsymbol{s}}) = \mathrm{e}^{-\mathrm{i}k\hat{\boldsymbol{s}}_0\cdot\boldsymbol{r}}\gamma^*(\boldsymbol{r}_0, \boldsymbol{r})\,\mathrm{e}^{\mathrm{i}k\hat{\boldsymbol{s}}\cdot\boldsymbol{r}_0},$$

so that

$$I_\mathrm{coh} = |\gamma(\boldsymbol{r}_0, \boldsymbol{r})|^2\cos[(\boldsymbol{k}+\boldsymbol{k}_0)\cdot(\boldsymbol{r}-\boldsymbol{r}_0)].$$

By collecting these two results, one obtains the total intensity scattered in the direction $\boldsymbol{k}$ for an incident wave along $\boldsymbol{k}_0$:

$$I = I_\mathrm{inc}\{1+\cos[(\boldsymbol{k}+\boldsymbol{k}_0)\cdot(\boldsymbol{r}-\boldsymbol{r}_0)]\}. \tag{8}$$

This expression calls for some remarks. First, the part associated with the second phase-dependent term gives rise to a strong anisotropy in the angular dependence of the average intensity, around the backscattering direction $\boldsymbol{k} = -\boldsymbol{k}_0$, where one has a value *exactly twice* the incoherent intensity. Secondly, this phase-dependent factor remains only in the multiple scattering situation, i.e., the factor 2 does not appear for single scattering. This coherent term is based on the last symmetry still present in the medium: the time reversal symmetry. If θ is the relative angle between $\hat{\boldsymbol{s}}$ and $\hat{\boldsymbol{s}}_0$, then the coherence on a given sequence is lost for θ larger than $\lambda/|\boldsymbol{r}-\boldsymbol{r}_0|$. Since the average value of $|\boldsymbol{r}-\boldsymbol{r}_0|$ for the shortest sequence of multiple scattering is the mean distance between two scattering events, i.e. the elastic mean free path l, one expects the total intensity *$I(\theta)$ to increase by up to a factor 2 inside a cone of angular width $\lambda/2\pi l$.* This interference effect is now well known, and is on the basis of the weak localization correction in electronic systems (Course 4 by Ramakrishnan). But the transport coefficients in the bulk, like for example the conductivity, are given by an angular integration of $I(\theta)$, which hides the angular dependence and the cone of coherent backscattering to give only a correction proportional to the volume of this cone. Our aim now is to describe a situation where it is possible to obtain the full angular dependence. This can be realized by the study of the light reflected by a semi-infinite disordered medium (or more generally any bounded medium), since the phase shift between the interfering paths remains fixed when light emerges from the disordered medium.

4. The lineshape of the albedo

We consider here the problem of the average intensity reflected by a semi-infinite disorder medium as a function of the angle [7] (fig. 3). And we define the albedo $\alpha(\hat{s}_0, \hat{s})$ as the ratio of the emergent energy flux per unit solid angle $\mathrm{d}\Omega$ around the direction $\hat{s}$ to the incident energy flux around the direction $\hat{s}_0$. $\alpha(\hat{s}_0, \hat{s})$ is given by [7]

$$\alpha(\hat{s}_0,\hat{s}) = \frac{c}{4\pi l^2}\int \mathrm{d}z\, \mathrm{d}z'\, \mathrm{d}^2\rho\, \mathrm{d}t\, \mathrm{e}^{-z/\mu_0 l - z'/\mu l}$$

$$\times \{1+\cos[k(\hat{s}+\hat{s}_0)\cdot(\boldsymbol{r}-\boldsymbol{r}')]\}\, P(r, r'; t). \tag{9}$$

In this expression, μ and μ_0 are, respectively, the projections of $\hat{s}$ and $\hat{s}_0$ on the z-axis, while $\boldsymbol{\rho}$ is the projection of $\boldsymbol{r}-\boldsymbol{r}'$ on the interface plane.

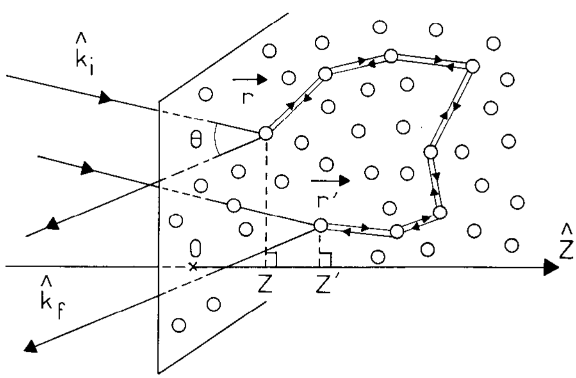

Fig. 3. Geometry used for the calculation of the coherent albedo, showing two interfering light paths.

Let us note that we have omitted the single scattering contribution in eq. (9) since it is not affected by the interference effect. Of course, for a quantitative comparison with experiments we must take this contribution into account.

To go further we need some assumptions in order to calculate the Green's function $P(r, r'; t)$. This question has been studied extensively in classical transport theory (see, e.g., ref. [4]). For the radiative transfer equation it can be shown that, far enough from the interface, $P(r, r'; t)$ is a solution of a time-dependent diffusion equation, which means that in the limit of long time (compared to the elastic scattering time τ) and long distances (compared to the elastic mean free path l), the light intensity has a brownian motion in the disordered medium. $P(r, r'; t)$ is therefore the probability distribution of a random walk between points $\boldsymbol{r}$ and $\boldsymbol{r}'$ during the time t, which never crosses the interface. This last boundary condition is satisfied by cancelling the probability P on the plane $z=-z_0$, where the value $z_0=0.7104\cdots l$ is obtained exactly for the stationary case of scattering by point-like scatterers. This value of z_0 will be particularly well adapted for the study of the stationary albedo [7]. But for the time-dependent case, we suppose at least qualitatively that $z_0=0.71\ l$ is a good approximation for the calculation of $P(r, r'; t)$, which is therefore given by

$$P(r, r'; t)=\frac{1}{(4\pi Dt)^{d/2}}\,\mathrm{e}^{-\rho^2/4Dt} \times\{\exp[-(z-z')^2/4Dt]-\exp[-(z+z'+2z_0)^2/4Dt]\}. \tag{10}$$

In this relation the translational invariance of the average medium along the x and y directions imposes that P depends only on $\rho=|(\boldsymbol{r}-\boldsymbol{r}')_\perp|$, while the terms in braces due to the image select only the diffusion paths not crossing the interface plane. Let us also note that in expression (10) for $P(r, r'; t)$ we use $D=\frac{1}{3}lc$ for the diffusion constant. Therefore we have not taken into account the renormalization of D due to weak localization effects. In a three-dimensional system, it gives a relative correction of order $(\lambda/l)^2$. Since we are interested here in an effect of the order of λ/l, we shall neglect this renormalization. When one approaches the Anderson mobility edge, this assumption must obviously be considered [8].

Finally, we calculate the analytic expression for the albedo in order to compare it with the quantum correction to the electronic diffusion constant. Let us simplify the expression for P. In the asymptotic regime for long time, we can write

$$P(\rho, z, z'; t) \simeq \frac{(l+z_0)^2}{(4\pi)^{d/2}} \frac{e^{-\rho^2/4Dt}}{(Dt)^{d/2+1}}. \tag{11}$$

Therefore, the coherent part of the albedo is nothing but the two-dimensional Fourier transform of a random walk parallel to the interface, or the small-angle "structure factor" of the fluctuations of the light intensity at characteristic length $2\pi/k_\perp$ after a time t,

$$\alpha_c(k_\perp, t) \cong \frac{c(l+z_0)^2}{(4\pi Dt)^{d/2+1}} \int d^2\rho \, e^{-\rho^2/4Dt} \, e^{ik_\perp \cdot \rho}, \tag{12}$$

or

$$\alpha_c(k_\perp) = \frac{c(l+z_0)^2}{4(4\pi)^{d/2-1}} \int_\tau^\infty dt \frac{e^{-Dtk_\perp^2}}{(Dt)^{3/2}}. \tag{13}$$

The most remarkable feature now is that $a_c(k_\perp)$ is, apart from a constant factor, independent of the space dimensionality d. Therefore, the two-dimensional albedo behaves exactly as in three dimensions since the presence of the interface destroys the recurrence of the random walk.

Expression (13) given above for $\alpha_c(k_\perp)$ contains all the physical features of the albedo. First, for $k_\perp = 0$ we recover the factor two between the coherent and incoherent parts. Second, for small angle θ, or $k_\perp \simeq 2\pi\theta/\lambda$ around the backscattering direction, the exponential in eq. (13) introduces a cut-off $t_c = \lambda^2/4\pi D\theta^2$ in the integral and gives finally the observed [7] triangular shape of the albedo:

$$\alpha(\theta) = \alpha(0)[1 - (l+z_0)k_\perp + O(k_\perp^2)]. \tag{14}$$

The quite unusual triangular lineshape around the backscattering direction can be understood as follows [9]. Let us use, instead of the time t, the perimeter n of the random walk path of the light such that $n = t/\tau$. Therefore, the coherent part of the albedo can be written as the series

$$\alpha_c(k_\perp) \propto \sum_{n=0}^{\infty} \frac{e^{-n(\theta/\theta_0)^2}}{n^{3/2}}, \tag{15}$$

where $\theta_0 = \lambda/2\pi l$. The coherent peak, therefore, appears as the superposition of the contributions of all the coherent multiple scattering paths of length n. This cumulative contribution of gaussian peaks gives the triangular singularity at $\theta = 0$. An interesting parallel can be established between eq. (15) for $\alpha_c(k_\perp)$ and the relation between the average number of noncondensed bosons $\bar{N}$ and the chemical potential μ for an ideal Bose gas, if one replaces $\bar{N}\lambda^3/V$ by α_c and β by $-(\theta/\theta_0)^2$, respectively. The triangular singularity then corresponds to the divergence of the compressibility ($\propto \partial\bar{N}/\partial\mu$) as the Bose–Einstein condensation is approached ($\mu \to 0$).

Any physical cut-off, like the absorption length L in a finite-frequency experiment, will be responsible of a rounding effect in the lineshape as in the case of the finite-size effect at the critical temperature of a phase transition.

Expression (13) of the albedo must be compared with the formula for the quantum correction to the diffusion constant (see Course 4, which is proportional to

$$\frac{\delta D}{D} \propto c\lambda^{d-1} \int_\tau^\infty \frac{\mathrm{d}t}{(Dt)^{d/2}}, \tag{16}$$

which diverges in two dimensions, in contrast to the albedo as mentioned previously. The prefactor $(\lambda/l)^{d-1}$ obtained after the integration can be justified simply by considering the solid angle of the cone aperture for coherent backscattering. The enhancement by the factor 2 right at the backscattering direction leads to an increase of the cross section and finally to the diminution of the diffusion constant.

5. Polarization effect

The electromagnetic field has been treated so far as a scalar field. This is often justified by the simple idea that the multiple scatterings strongly depolarize the incident light. This is not true and it has been discovered [2, 7, 10] that the peak lineshape depends on the polarization of the light. The previous analysis works very well for peaks measured in a parallel configuration. But for crossed polarizers, the shape is rounded and the maximum at $\theta = 0$ is much less than 2. These findings can be explained by considering the vectorial form of Rayleigh scattering [7, 9, 10]. Simple geometrical considerations show that the projections of the emerging electric field on the incident direction of the polarization for the direct multiply scattered wave and the reversed one are equal. This result justifies the previous scalar treatment. But for a crossed-polarizer configuration the situation is a bit more complicated. The coherence ratio $\langle p_{n\perp} p'_{n\perp}\rangle / \langle p^2_{n\perp}\rangle$ between two sequences of n-multiple scattering decreases exponentially with n for $\theta = 0$. This attenuation is equivalent to an absorption effect and is responsible of the rounding effect observed in the crossed configuration. A complete analysis of the polarization effect has been given within the diffusion approximation in two recent articles [9, 10].

6. Conclusion

In this seminar, we have presented physical arguments to explain both coherent backscattering and weak localization phenomena in optics and in metals. They both originate from the last coherence effect which survives in the presence of complete disorder. However, they differ by the fact that the coherent contribution to the albedo comes from all the diffusion paths starting and ending on the interface plane, while the quantum correction to the electrical conductivity comes from the closed diffusion loops measuring the return probability. From this difference comes the strong space dimensionality dependence of $\delta D/D$, which is absent in the albedo. This last fact is specific to the presence of an interface and could not be obtained from bulk considerations.

The triangular singularity of the albedo around the backscattering direction results from the addition of all contributions of nth order multiple scattering, and it can be reached only in the limit of n going to infinity. Any process which introduces a limitation on the order n of the multiple scattering or, in other words, on the total length of the random paths will round the peak [9]. The coherent backscattering effect therefore appears as a probe to sample the perimeter of the loops. This is an improvement compared with the electronic case, for which the quantum correction $\delta D/D$ gives only the amount of energy contained in the backscattering cone. Furthermore, since the peak lineshape gives direct information on the transport in a random medium, an extension [9] of this analysis towards non-Euclidian random walks is of great interest.

Acknowledgement

It is a pleasure to thank Georg Maret for fruitful and interesting discussions.

References

[1] A.A. Golubentsev, Sov. Phys. - JETP 59 (1984) 26;
E. Akkermans and R. Maynard, J. Physique Lett. 46 (1985) L1045.

[2] Y. Kuga and A. Ishimaru, J. Opt. Soc. Am. A 8 (1984) 831;
M.P. van Albada and A. Lagendijk, Phys. Rev. Lett. 55 (1985) 2692;
P.E. Wolf and G. Maret, Phys. Rev. Lett. 55 (1985) 2696.
[3] S. Etemad, R. Thomson and M.J. Andrejco, Phys. Rev. Lett. 57 (1986) 575;
M. Kaveh, M. Rosenbluh, I. Edrei and I. Freund, Phys. Rev. Lett. 57 (1986) 2049.
[4] A. Ishimaru, Wave Propagation and Scattering in Random Media, Vol. 1 (Academic Press, New York, 1978).
[5] S. Washburn and R.A. Webb, Adv. Phys. 35 (1986) 375.
[6] A.I. Larkin and D.E. Khmelnitskii, Sov. Phys. - Usp. 25 (1982) 185.
[7] E. Akkermans, P.E. Wolf and R. Maynard, Phys. Rev. Lett. 56 (1986) 1471.
[8] P.W. Anderson, Philos. Mag. B 52 (1985) 505.
[9] E. Akkermans, Thesis, Univ. of Grenoble (June 1986);
E. Akkermans, G. Maret, R. Maynard and P.E. Wolf, to be published.
[10] M.J. Stephen and G. Cwillich, Phys. Rev. B 34 (1986) 7564.